

## A GIANT FLARE FROM A SOFT GAMMA REPEATER IN THE ANDROMEDA GALAXY (M31)

E. P. MAZETS,<sup>1</sup> R. L. APTEKAR,<sup>1</sup> T. L. CLINE,<sup>2</sup> D. D. FREDERIKS,<sup>1</sup> J. O. GOLDSTEN,<sup>3</sup> S. V. GOLENETSKII,<sup>1</sup>  
K. HURLEY,<sup>4</sup> A. VON KIENLIN,<sup>5</sup> AND V. D. PAL'SHIN<sup>1</sup>

Received 2007 December 7; accepted 2008 March 1

### ABSTRACT

The light curve, energy spectra, energetics, and IPN localization of an exceedingly intense, short-duration, hard-spectrum burst, GRB 070201, obtained from *Konus-Wind*, *INTEGRAL* (SPI-ACS), and *MESSENGER* data are presented. The total fluence of the burst and the peak flux are  $S = 2.00^{+0.10}_{-0.26} \times 10^{-5}$  erg cm<sup>-2</sup> and  $F_{\max} = 1.61^{+0.29}_{-0.50} \times 10^{-3}$  erg cm<sup>-2</sup> s<sup>-1</sup>. The IPN error box has an area of 446 arcmin<sup>2</sup> and covers the peripheral part of the M31 galaxy. Assuming that the source of the burst is indeed in M31 at a distance of 0.78 Mpc, the measured values of the fluence  $S$  and maximum flux  $F_{\max}$  correspond to a total energy of  $Q = 1.5 \times 10^{45}$  erg and a maximum luminosity  $L = 1.2 \times 10^{47}$  erg s<sup>-1</sup>. These data are in good agreement with the corresponding characteristics of the previously observed giant flares from other soft gamma repeaters. The evidence for the identification of this event as a giant flare from a soft gamma repeater in the M31 galaxy is presented.

*Subject headings:* gamma rays: bursts — stars: neutron

### 1. INTRODUCTION

Soft gamma repeaters (SGRs) are a special rare class of strongly magnetized neutron stars exhibiting two types of gamma-ray burst emission. Occasionally, SGRs enter an active stage and emit repeated short bursts with spectra which, in an energy range above 10–15 keV, can be approximated by a soft thermal bremsstrahlung-like function with  $kT \approx 20$ –30 keV. The bursting activity may last from several days to a year or more, followed by a long quiescent period lasting up to several years.

Much more rarely, perhaps once every 30–40 yr, an SGR may emit a giant flare (GF) with enormous intensity. The energy released in such a flare in gamma rays is comparable to the total energy emitted by the Sun over  $10^4$ – $10^5$  yr or more. GFs display short ( $\sim 0.2$ – $0.5$  s) initial pulses of hard gamma rays with a steep leading edge and a more extended trailing edge which, as a rule, evolves into a soft, long-decaying tail pulsating with the neutron star rotation period. A GF is frequently preceded by a pronounced increase in bursting activity (Frederiks et al. 2007a).

The first two SGRs were discovered and localized in 1979 March by the *Konus* experiment on *Venera* 11 and 12. A GF from SGR 0526–66 was detected on 1979 March 5 by numerous spacecraft (Mazets et al. 1979a; Evans et al. 1980; Cline et al. 1980). One of the first results of the interplanetary network (IPN) was the localization of the first GF to an error box inside the N49 supernova remnant in the Large Magellanic Cloud (LMC; Cline et al. 1980). Another important result was the observation and localization by the *Konus* experiment of  $\sim 17$  weak, soft recurrent bursts emitted by SGR 0526–66 in the years following the GF (Mazets et al. 1979a; Golenetskii et al. 1984). Moreover, in 1979 March, *Konus* detected and localized three similar recurrent bursts from another source, SGR 1900+14 (Mazets et al. 1979b). The third SGR, 1806–20, was discovered in 1983 (Laros et al. 1987;

Atteia et al. 1987; Kouveliotou et al. 1987) and the fourth, SGR 1627–41, in 1998 (Hurley et al. 1999b; Woods et al. 1999). It has become clear that SGRs are very rare astrophysical objects. The GF on 1979 March 5 remained a unique event for 20 years, until new GFs were detected from SGR 1627–41 on 1998 June 18 (Mazets et al. 1999a) and from SGR 1900+14 on 1998 August 27 (Hurley et al. 1999a; Feroci et al. 1999; Mazets et al. 1999b). Finally, a GF from SGR 1806–20 on 2004 December 27 was also observed (Hurley et al. 2005; Frederiks et al. 2007a). The extremely high intensity of the initial pulses of the GFs suggested that these events could be detected in galaxies at distances up to 10–30 Mpc.

The short, hard GRB 051103 was localized by the IPN to the nearby M81 group of interacting galaxies, which lies at a distance of 3.6 Mpc (Golenetskii et al. 2005). The possibility of identifying this burst as a GF from an SGR in the M81 group, as opposed to a short GRB in a background galaxy, has been discussed (Frederiks et al. 2007b; K. Hurley et al. 2008, in preparation; Ofek et al. 2007).

On 2007 February 1 *Konus-Wind* recorded a short-duration, hard-spectrum gamma-ray burst which had a higher intensity than any previously observed event. The burst was localized by the IPN (Golenetskii et al. 2007). The final localization (a 446 arcmin<sup>2</sup> error box) covers the outer arms of the M31 galaxy. The analysis presented below of the time history, spectral characteristics, and energetics argues strongly for the interpretation that this event is actually a GF from an SGR in the Andromeda galaxy. In a companion paper, Abbott et al. (2008) discuss the LIGO data taken at the time of this event. In Ofek et al. (2008), the optical and X-ray content of the error box are discussed.

### 2. OBSERVATIONS AND LOCALIZATION

The light curve of GRB 070201 (*Konus* trigger time  $T_0 = 55,390.780$  s UT, corresponding to an Earth-crossing time of 55,390.261 s), recorded by the *Konus-Wind* S2 detector in the energy range 17–1130 keV, is shown in Figure 1. It displays a narrow pulse with a rather steep leading edge ( $\sim 20$  ms) followed by more prolonged decay to  $T - T_0 \approx 180$  ms. The maximum count rate occurs in a  $\leq 2$  ms long interval. The burst profile is not smooth; in most cases, the variations evident in the count rate at the top of the pulse and in its decay phase are statistically

<sup>1</sup> Ioffe Physico-Technical Institute of the Russian Academy of Sciences, St. Petersburg 194021, Russia.

<sup>2</sup> NASA Goddard Space Flight Center, Greenbelt, MD 20771.

<sup>3</sup> Applied Physics Laboratory, The Johns Hopkins University, Baltimore, MD 20723.

<sup>4</sup> Space Sciences Laboratory, University of California at Berkeley, Berkeley, CA 94720-7450.

<sup>5</sup> Max-Planck-Institut für extraterrestrische Physik, D-85741 Garching, Germany.

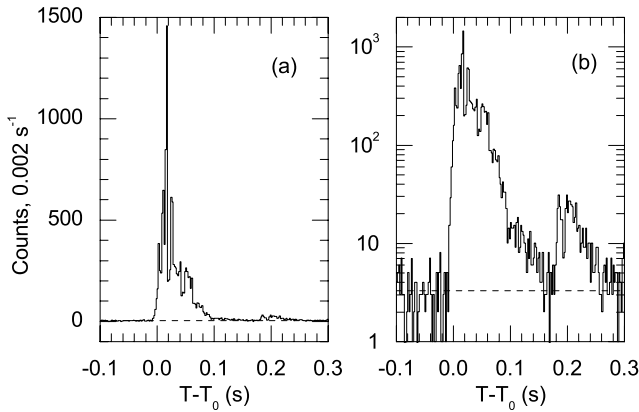


FIG. 1.—The 17–1130 keV *Konus-Wind* light curve of GRB 070201 (dead-time corrected) at the highest available time resolution (2 ms), presented (a) on a linear count rate scale and (b) on a logarithmic scale to enhance the low-intensity portions.

significant. A weak secondary flash is observed at  $T - T_0 \approx 180$ –280 ms. Comparison of the light curves in three energy bands, G1 (17–70 keV), G2 (70–300 keV), and G3 (300–1130 keV; Fig. 2), and of the hardness ratios G2/G1 and G3/G2 reveals a strong, rapid spectral evolution of the radiation. The most pronounced changes are observed for the high-energy part of the spectrum (energies  $E_\gamma > 300$  keV). The duration of the high-energy radiation does not exceed 80 ms. The second, weak rise

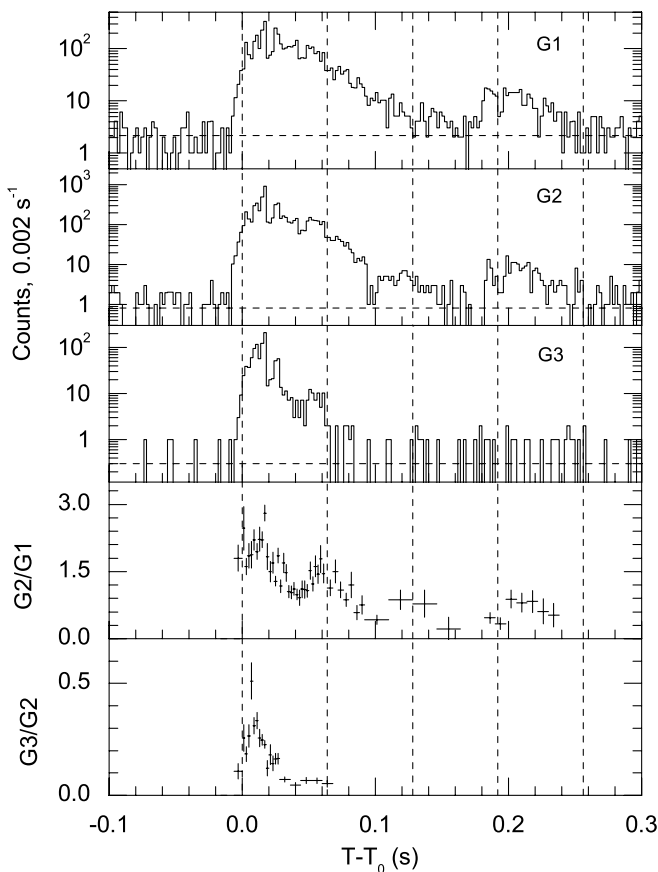


FIG. 2.—*Konus-Wind* light curve in three energy bands, G1 (17–70 keV), G2 (70–300 keV), and G3 (300–1130 keV), and the hardness ratios G2/G1 and G3/G2. The dashed lines indicate the four successive 64 ms intervals where the energy spectra were measured.

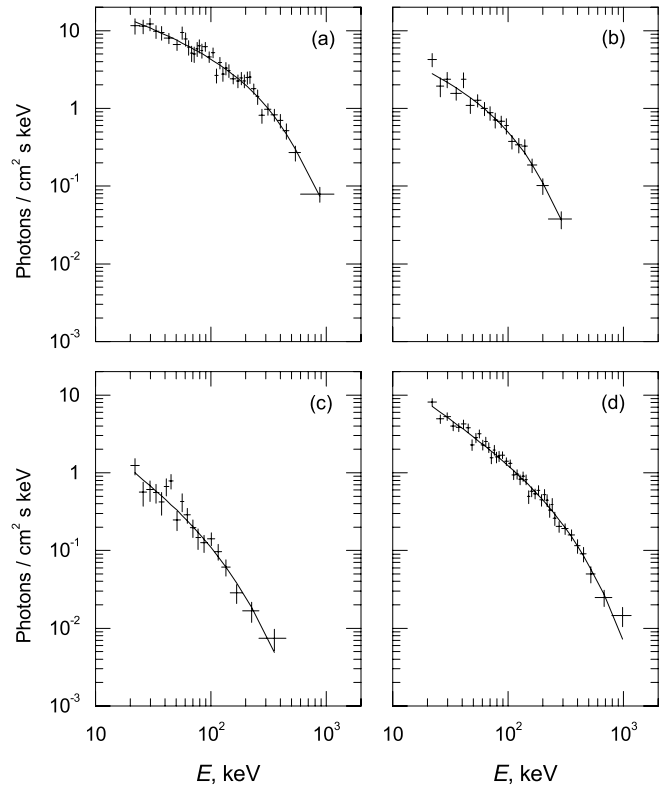


FIG. 3.—Deconvolved photon spectra of the burst accumulated over the ( $T - T_0$ ) intervals (a) 0–64 ms, (b) 64–128 ms, (c) 128–256 ms, and (d) the time-integrated spectrum 0–256 ms.

in intensity at  $T - T_0 \approx 180$  ms is present only for the soft part of the spectrum at energies  $E_\gamma < 300$  keV. Four multichannel spectra were measured in the course of the burst, each with an accumulation time of 64 ms. They cover the energy range from 17 keV to 14 MeV, but no statistically significant emission is seen above 2 MeV. The boundaries of the successive accumulation intervals  $N = 1, 2, 3$ , and 4 are shown in Figure 2 (*dashed lines*). Because of the small number of counts in interval 3, spectra 3 and 4 were combined. The time-integrated spectrum of the entire burst was accumulated over the interval 0–256 ms. The raw count rate spectra were rebinned in order to have at least 20 counts per energy bin and then fitted using XSPEC, version 11.3 (Arnaud 1996). The detector response function was calculated specifically for the  $55.9^\circ$  burst incidence angle, determined from the IPN localization data.

A good fit was obtained for a power-law spectrum with an exponential cutoff,  $dN_{\text{ph}}/dE \propto E^{-\alpha} \exp[-(2 - \alpha)E/E_p]$ , where  $E_p$  is the peak energy in the  $EF(E)$  spectrum. We also tested the Band et al. (1993) gamma-ray burst model, but no statistically significant high-energy power-law tail was found in any fitted spectrum. The deconvolved photon spectra for intervals 1, 2, and 3+4, and for the time-integrated spectrum of the burst, are shown in Figure 3, and the spectral parameters are summarized in Table 1. Comparison of the  $E_p$  values shows that the spectrum for interval 1 is the hardest. Returning to Figure 2, note that the accumulation time of this spectrum is rather long (64 ms) compared to the characteristic evolution time; hence, the spectrum is strongly time-averaged. Most of the high-energy photons are accumulated during the first  $\sim 20$  ms. This remarkable fact means that the flux of photons with the hardest spectrum is emitted near the peak of the initial pulse. The burst fluence in the 20 keV–1.2 MeV range is  $2.00^{+0.10}_{-0.26} \times 10^{-5}$  erg  $\text{cm}^{-2}$ . The 2 ms peak flux measured from

TABLE 1  
SUMMARY OF SPECTRAL FITS

Time Interval (s)	$\alpha$	$E_p$ (keV)	$\chi^2/\text{dof}$
0–0.064	$0.52^{+0.13}_{-0.15}$	$360^{+44}_{-38}$	31.6/35
0.064–0.128	$0.56^{+0.38}_{-0.42}$	$128^{+24}_{-16}$	11.3/15
0.128–0.256	$1.06^{+0.52}_{-0.52}$	$123^{+54}_{-25}$	19.3/16
0–0.256	$0.98^{+0.10}_{-0.11}$	$296^{+38}_{-32}$	39.7/40

$T_0 + 0.016$  s in the same energy band is  $1.61^{+0.29}_{-0.50} \times 10^{-3}$  erg  $\text{cm}^{-2} \text{s}^{-1}$ . All the uncertainties are for the 90% confidence level.

GRB 070201 was detected by *Wind* (Konus) with a time resolution of up to 2 ms, by *INTEGRAL* (SPI-ACS) with a resolution of 50 ms, by the *MESSENGER* (Mercury Surface, Space Environment, Geochemistry, and Ranging) Gamma-Ray and Neutron Spectrometer (Goldsten et al. 2007) with a resolution of 1 s, and by the *Swift* BAT with a resolution of 1 s (outside the coded field of view; J. Cummings 2007, private communication). The initial triangulation was given in Hurley et al. (2007). The coordinates of the center and vertex of the refined  $446 \text{ arcmin}^2$   $3\sigma$  error box are listed in Table 2. The center lies  $\sim 1^\circ$  away from the center of M31. Assuming that the source of GRB 070201 is situated in M31 at a distance of 0.78 Mpc, the measured values of the fluence and peak flux correspond to an isotropic energy output  $Q = 1.5 \times 10^{45}$  erg and an isotropic peak luminosity  $L = 1.2 \times 10^{47}$  erg  $\text{s}^{-1}$ .

The relative proximity of M31 makes it worthwhile to search for the afterglow of GRB 070201 in soft gamma rays, i.e., the tail of the possible GF. While recording a burst in the trigger mode with high time resolution, Konus also continues to measure the count rates in each of the detectors, S1 and S2, in four energy windows, G1, G2, G3, and Z (a charged-particle channel), in background mode with a time resolution of 2.944 s. The initial pulse of GRB 070201 falls completely into a single 2.944 s interval around  $T_0$ . We began by selecting a long series of count rate data, excluding this interval. Then, in order to suppress fast statistical fluctuations we formed a new series consisting of a sum over 94.2 s ( $32 \times 2.944$  s), which can originate at the beginning of any 2.944 s interval. Two such series, in the energy bands G1 and G2, are shown in Figures 4a and 4b; they are synchronized to the first 2.944 s interval following the excluded one. The position of the excluded interval is marked by a vertical line. The discontinuity at  $T - T_0 \sim 240\text{--}3800$  s is due to the transfer of the accumulated data to the onboard memory. A significant increase in the count rate ( $4.3\sigma$  above the average background level) is seen only in the soft energy band G1 and only for the first large

TABLE 2  
IPN ERROR BOX OF GRB 070201

Center/Intersection	R.A. (J2000.0)	Decl. (J2000.0)
Center	00 44 32	+42 14 21
Vertex		
1	00 46 18	+41 56 42
2	00 41 51	+42 52 08
3	00 42 47	+42 31 41
4	00 47 14	+41 35 35

NOTE.—Units of right ascension are hours, minutes, and seconds, and units of declination are degrees, arcminutes, and arcseconds.

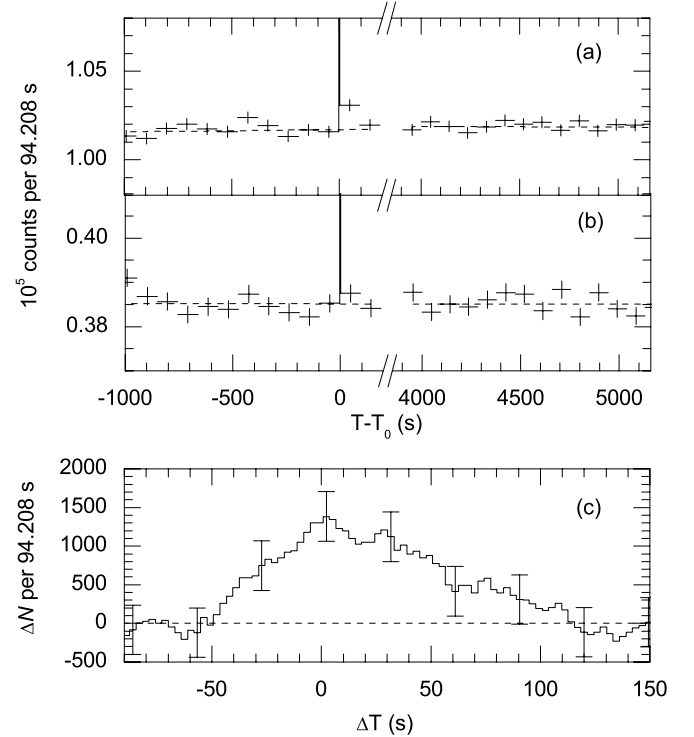


FIG. 4.—Waiting mode count rates  $N$  in the energy bands (a) G1 and (b) G2, averaged over 94.208 s intervals (excluding the burst). For G1, the first interval after  $T_0$  exhibits a count excess  $\Delta N$  of  $4.3\sigma$  above the average background level. Panel c shows how this excess  $\Delta N$  varies if the beginning of the 94.208 interval is shifted by an interval  $\Delta T$  forward or backward from  $T_0$  step-by-step, with  $\Delta T = 2.944$  s.

interval after  $T_0$ . Figure 4c shows how the excess counts  $\Delta N$  vary if the beginning of the 94.2 s interval is shifted forward or backward from  $T_0$  step-by-step by 2.944 s. The dependence of  $\Delta N$  on the time shift  $\Delta T$  implies that the gradually decreasing soft gamma-ray flux is indeed present in each 2.944 s interval after  $T_0$  but is absent prior to it. This important result confirms the detection of the decaying soft afterglow of GRB 070201. For an optically thin thermal bremsstrahlung spectrum with  $kT \approx 30$  keV, the 94.2 s count excess  $\Delta N = 1385 \pm 320$  corresponds to a fluence  $S \approx 1 \times 10^{-6}$  erg  $\text{cm}^{-2}$ . Assuming that we are observing emission in the tail of a GF from M31, its energy is  $Q_{\text{tail}} \approx 7 \times 10^{43}$  erg.

### 3. DISCUSSION

The Andromeda galaxy (M31), as the closest massive galaxy, has long been regarded as one of the most likely candidates for searching for observable GFs from distant extragalactic SGRs (Mazets et al. 1999b; Bisnovaty-Kogan 1999). It is well known that one of the dominant features of the structure of M31 is a bright circular ring with a radius of 10 kpc, discovered by Arp (1964) in  $H\alpha$  observations. In agreement with numerous observations, the ring reveals the main star formation region of the galaxy. In the far-infrared, the first *IRAS* images of M31 also revealed a bright circular ring (Habing et al. 1984). The close correspondence between the details of the  $H\alpha$  and far-infrared images of the galaxy implies that the radiation of massive hot stars (Devereux et al. 1994) is the common energy source of these emissions. Recently, high spatial resolution images of M31 have been obtained in the mid- and far-infrared at different wavelengths with the *Spitzer Space Telescope* (Barmby et al. 2006; Gordon et al. 2006) and in the far- and near-ultraviolet with *GALEX*

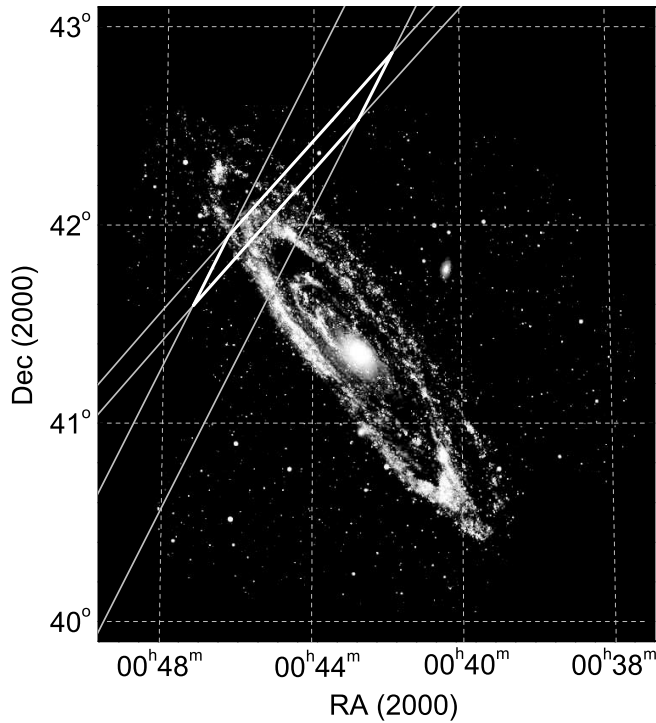


FIG. 5.—UV image of the M31 galaxy (Thilker et al. 2005) and the  $3\sigma$  IPN error box of GRB 070201.

(Thilker et al. 2005). These very similar images clearly show the central region, the fragmented spiral arms, the main circular ring with  $R \approx 10$  kpc, and a less luminous outer ring with  $R \approx 14$  kpc.

Figure 5 shows the ultraviolet image of M31 (Thilker et al. 2005). The IPN error box overlaps the northeastern part of the galaxy. It contains segments of both the  $R \approx 10$  kpc ring and of the weaker  $R \approx 14$  kpc outer ring. The probability of a chance overlapping of the error box and the image is rather low ( $\sim 10^{-4}$ ). Twenty-two sources from an *XMM-Newton* X-ray survey of M31 (Pietsch 2005) fall within the error box. Among these, two sources are active galactic nuclei, and five are foreground objects. (See Ofek et al. [2008] for a more complete analysis.) SGRs in the quiescent state are typically sources of pulsating soft X-rays with an average 0.5–10 keV luminosity of  $10^{35}$ – $10^{36}$  erg s $^{-1}$  and a spectrum which can be described as a combination of a blackbody and a power law (Kulkarni et al. 2003; Hurley et al.

2000; Kouveliotou et al. 2001). Spectral studies of the unidentified soft X-ray sources in the error box, which could be SGRs in M31, would clearly be important.

We now examine additional evidence which strengthens the interpretation of the 2007 February 1 event as a GF from an SGR in M31. This comes from a comparison of the energetics, time history, and spectral behavior of GRB 070201 with the corresponding characteristics of the previously observed GFs on 1979 March 5 (SGR 0526–66), 1998 June 18 (SGR 1627–41), 1998 August 27 (SGR 1900+14), and 2004 December 27 (SGR 1806–20). Here we are mainly interested in the characteristics of the GF initial pulses, but unfortunately, it is just this information which is the hardest to obtain reliably. When a sensitive gamma-ray detector records an initial pulse with an immense intensity, it is strongly overloaded, which makes it difficult or even impossible to obtain information about the main part of the peak. If a giant pulse is recorded by detectors of low-energy charged particles which have low sensitivity to gamma rays, there is no saturation problem in most cases. However, severe difficulties are encountered instead when measuring the photon energy, obtaining spectra, and consequently deriving energy estimates. Nevertheless, the entire set of data on initial pulses, obtained both with gamma-ray spectrometers (Mazets et al. 1979a, 1982, 1999a; Hurley et al. 1999a; Frederiks et al. 2007a) and with charged-particle detectors (Hurley et al. 2005; Palmer et al. 2005; Terasawa et al. 2005; Schwartz et al. 2005; Tanaka et al. 2007), can be used to establish the general pattern of the initial pulse.

We restrict this comparison of GFs to a limited number of their characteristics for the following reasons. The time structure of the initial pulse is likely to be very complex. The profile of both the steep leading edge of the pulse, as in SGR 1806–20 (Palmer et al. 2005), and its more prolonged decay, as in SGR 1900+14 (Tanaka et al. 2007), contain significant intensity variations on both short and long timescales. Among other things, the appearance of the light curve will be strongly affected by the spectral variability of the emission. At high count rates close to saturation level, dead-time and pileup corrections of light curves and energy spectra are difficult, if not impossible. Therefore, we include in Table 3 only two fairly reliable characteristics of the initial pulse,  $t_R$  and  $E_p$ ;  $t_R$ , the rise time, is the time between the detection of hard gamma radiation above the background and the peak of the initial pulse, and  $E_p$  is the photon energy at the maximum of the time-integrated  $EF(E)$  spectrum of the pulse. Table 3 also contains data on the peak luminosity  $L_{\max}$  and the energy release  $Q$  of the initial pulses, as well as the energy in the GF tails  $Q_{\text{tail}}$ . In keeping

TABLE 3  
SOME CHARACTERISTICS OF KNOWN GIANT FLARES

Parameter	SGR 0526–66 <sup>a</sup> (LMC)	SGR 1627–41 <sup>b</sup>	SGR 1900+14 <sup>c</sup>	SGR 1806–20 <sup>d</sup>	SGR 0952+69 <sup>e</sup> (M81)	SGR 0044+42 <sup>f</sup> (M31)
Date (YYMMDD).....	790305	980618	980827	041227	051103	070201
Distance (kpc).....	50	10	15	15	3600	780
Rise time, $t_R$ (ms).....	$\sim 25$	$\sim 15$	$\sim 15$	$\sim 25$	$\sim 6$	$\sim 20$
Peak energy, $E_p$ (keV).....	$\sim 500$	$\sim 150$	$> 250$	$\sim 850$	$\sim 900$	$\sim 300$
Luminosity, $L_{\max}$ (erg s $^{-1}$ ).....	$6.5 \times 10^{45}$	$3.4 \times 10^{44}$	$2.3 \times 10^{46}$	$3.5 \times 10^{47}$	$4.3 \times 10^{48}$	$1.2 \times 10^{47}$
Energy release, $Q$ (erg).....	$7 \times 10^{44}$	$1 \times 10^{43}$	$4.3 \times 10^{44}$	$2.3 \times 10^{46}$	$7 \times 10^{46}$	$1.5 \times 10^{45}$
Tail energy, $Q_{\text{tail}}$ (erg).....	$3.6 \times 10^{44}$	Absent	$1.2 \times 10^{44}$	$2.1 \times 10^{44}$	Not detected	$7 \times 10^{43}$

<sup>a</sup> The previous dead-time correction for the event (Mazets et al. 1979a, 1982) has been revised here, assuming that the initial pulse displays the expected strong hard-to-soft spectral evolution. This resulted in a reduction in  $t_R$  and an increase in  $L_{\max}$  and  $Q$ .

<sup>b</sup> Mazets et al. (1999a) and Aptekar et al. (2001).

<sup>c</sup> Tanaka et al. (2007), Hurley et al. (1999a), and Mazets et al. (1999b).

<sup>d</sup> Palmer et al. (2005) and Frederiks et al. (2007a).

<sup>e</sup> Frederiks et al. (2007b).

<sup>f</sup> This work.

with tradition, we suggest the same nomenclature for extragalactic and galactic SGRs, namely, SGR followed by the coordinates ( $\alpha$ ,  $\delta$ ) of the center of the error box.

Table 3 shows that estimates of both the luminosities and energy outputs in GFs are spread over a range of several orders of magnitude. On the other hand, the values of  $Q_{\text{tail}}$  are practically equal. Thus, it is particularly significant that the afterglow of GRB 070201 is similar to those of the other SGRs. A small spread in SGR  $Q_{\text{tail}}$  values implies similar magnetic field strengths from confinement arguments (Thompson & Duncan 1995). The only exception so far is the absence of a tail in GF 980618 from SGR 1627–41, which is probably caused by the relative weakness of

the magnetic field or its orientation. On the whole, Table 3 clearly demonstrates that both the temporal and energetic characteristics of the event on 2007 February 1 match the general pattern of a GF very closely. Beyond a doubt, we can conclude that this event is a GF which originated in SGR 0044+42 in M31.

On the Russian side, this work was supported by the Federal Space Agency of Russia and RFBR grant 06-02-16070. K. H. is grateful for IPN support under NASA grants NNG06GE69G (the *INTEGRAL* guest investigator program) and NNX07AR71G (*MESSENGER* Participating Scientist program).

## REFERENCES

- Abbott, B., et al. 2008, *ApJ*, 680, in press (arXiv: 0711.1163)  
 Aptekar, R. L., et al. 2001, *ApJS*, 137, 227  
 Arnaud, K. A. 1996, in *ASP Conf. Ser. 101, Astronomical Data Analysis Software and Systems V*, ed. G. Jacoby & J. Barnes (San Francisco: ASP), 17  
 Arp, H. 1964, *ApJ*, 139, 1045  
 Atteia, J.-L., et al. 1987, *ApJ*, 320, L105  
 Band, D., et al. 1993, *ApJ*, 413, 281  
 Barmby, P., et al. 2006, *ApJ*, 650, L45  
 Bisnovatyi-Kogan, G. S. 1999, preprint (astro-ph/9911275)  
 Cline, T., et al. 1980, *ApJ*, 237, L1  
 Devereux, N. A., et al. 1994, *AJ*, 108, 1667  
 Evans, W. D., et al. 1980, *ApJ*, 237, L7  
 Feroci, M., et al. 1999, *ApJ*, 515, L9  
 Frederiks, D. D., et al. 2007a, *Astron. Lett.*, 33, 1  
 ———. 2007b, *Astron. Lett.*, 33, 19  
 Goldsten, J., et al. 2007, *Space Sci. Rev.*, 131, 339  
 Golenetskii, S. V., et al. 1984, *Nature*, 307, 41  
 ———. 2005, *GCN Circ. 4197*, <http://gcn.gsfc.nasa.gov/gcn3/4197.gcn3>  
 ———. 2007, *GCN Circ. 6088*, <http://gcn.gsfc.nasa.gov/gcn3/6088.gcn3>  
 Gordon, K. D., et al. 2006, *ApJ*, 638, L87  
 Habing, H. J., et al. 1984, *ApJ*, 278, L59  
 Hurley, K., et al. 1999a, *Nature*, 397, 41  
 ———. 1999b, *ApJ*, 519, L143  
 ———. 2000, in *AIP Conf. Proc. 526, Gamma-Ray Bursts*, ed. R. M. Kippen, R. S. Mallozi, & G. F. Fishman (Melville: AIP), 763  
 Hurley, K., et al. 2005, *Nature*, 434, 1098  
 ———. 2007, *GCN Circ. 6103*, <http://gcn.gsfc.nasa.gov/gcn3/6103.gcn3>  
 Kouveliotou, C., et al. 1987, *ApJ*, 322, L21  
 ———. 2001, *ApJ*, 558, L47  
 Kulkarni, S. R., et al. 2003, *ApJ*, 585, 948  
 Laros, J. L., et al. 1987, *ApJ*, 320, L111  
 Mazets, E. P., Golenetskii, S. V., Guryan, Yu. A., & Ilyinskii, V. N. 1982, *Ap&SS*, 84, 173  
 Mazets, E. P., et al. 1979a, *Nature*, 282, 587  
 ———. 1979b, *Soviet Astron. Lett.*, 5, 343  
 ———. 1999a, *ApJ*, 519, L151  
 ———. 1999b, *Astron. Lett.*, 25, 635  
 Ofek, E., et al. 2007, *ApJ*, 659, 339  
 ———. 2008, *ApJ*, in press (arXiv: 0712.3585)  
 Palmer, D. M., et al. 2005, *Nature*, 434, 1107  
 Pietsch, W. 2005, *A&A*, 434, 483  
 Schwartz, S. J., et al. 2005, *ApJ*, 627, L129  
 Tanaka, Y. T., et al. 2007, *ApJ*, 665, L55  
 Terasawa, T., et al. 2005, *Nature*, 434, 1110  
 Thilker, D. A., et al. 2005, *ApJ*, 619, L67  
 Thompson, C., & Duncan, R. 1995, *MNRAS*, 275, 255  
 Woods, P. M., et al. 1999, *ApJ*, 519, L139